

## Secondary *UBVRI*-CCD standard stars in the neighbourhood of Landolt standard stars<sup>\*,\*\*</sup>

D. Galadí-Enríquez<sup>1,2</sup>, E. Trullols<sup>3,2</sup>, and C. Jordi<sup>2,4</sup>

<sup>1</sup> Centro de Astrobiología (CSIC-INTA), INTA Edif. S-18, Carretera de Ajalvir km 4, E-28850 Torrejón de Ardoz, Spain

<sup>2</sup> Dept. d'Astronomia i Meteorologia, Univ. de Barcelona, Avda. Diagonal 647, E-08028 Barcelona, Spain

<sup>3</sup> Dept. de Matemàtica Aplicada i Telemàtica, Univ. Politècnica de Catalunya, Avda. Victor Balaguer s/n, E-08800 Vilanova i la Geltrú, Spain

<sup>4</sup> Institut d'Estudis Espacials de Catalunya - IEEC, Edif. Nexus, Gran Capità 2-4, E-08034 Barcelona, Spain

Received April 13; accepted July 11, 2000

**Abstract.** A list of 681 *UBVRI* secondary standard stars for CCD photometry is presented. Visual magnitude ranges from 9.7 to 19.4, and the  $B - V$  colour index varies from 1.15 to 1.97. The stars are grouped into 11 different fields, each of them is generally observable in a single CCD frame. The stars are located near Landolt *UBVRI* equatorial standards, accessible to telescopes in both hemispheres, and mainly within the 5 – 8 hours range of right ascension. Photometry, equatorial coordinates and finding charts are provided.

**Key words:** methods: observational — techniques: photometric — stars: general

### 1. Introduction

One of the advantages of CCD photometry when compared to photoelectric detectors arises from the possibility of measuring more than one star simultaneously. This point is specially interesting in highly populated regions, as star clusters, where usually we are interested in several (or all) stars present in the CCD frame.

In order to transform instrumental CCD measurements to the standard system, it is necessary to observe a suitable set of standard stars. Quite often several stars

*Send offprint requests to:* D. Galadí-Enríquez

\* Based on observations made at the Centro Astronómico Hispano-Alemán and the Observatorio Astronómico Nacional in Calar Alto, Almería, Spain.

\*\* Full version of Table 4 is only available in electronic form at the CDS via anonymous ftp to cdsarc.u-strasbg.fr (130.79.128.5) or via <http://cdsweb.u-strasbg.fr/Abstract.html>

*Correspondence to:* dgaladi@am.ub.es

**Table 1.** Observational run and chip specifications

Period	Nov. 1991, Oct. 1993	Dec. 1993	Dec. 1994
Observatory	CAHA	OAN	CAHA
Telescope	1.23 m	1.52 m	1.23 m
Type:	GEC#10	THX 31156	TEK#6
Size (pixels):	385 × 576	1024 × 1024	1024 × 1024
Pixel size:	22 μm = 0.46''	19 μm = 0.33''	24 μm = 0.50''
Field of view:	3.0' × 4.4'	5.6' × 5.6'	8.6' × 8.6'
Gain:	5.7e <sup>-</sup> /ADU	3.5e <sup>-</sup> /ADU	4.3e <sup>-</sup> /ADU
RON:	2.3 ADU	2 ADU	1.5 ADU
Dyn. range:	65535 ADU	65535 ADU	65535 ADU
Linear up to:	40000 ADU	50000 ADU	45000 ADU
Bias level:	260 ADU	240 ADU	261 ADU
Overscan:	right-left	right-left	right-left

**Table 2.** Quantum efficiency of the detectors at the central wavelengths of *UBVRI* filters

Detector	wavelength (nm)				
	360	440	550	650	800
GEC#10	17%	19%	31%	49%	43%
TEK#6	50%	60%	65%	70%	60%
THX 31156	17%	15%	28%	38%	32%

are detected in the neighbourhood of a primary standard star, but they cannot be used in the reduction procedure due to the lack of standard photometry. So, the advantage arising from the two-dimensional character of CCD detectors is lost.

*UBVRI* standard stars by Landolt (1983, 1992) are widely used. They constitute an internally consistent and homogeneous realization of the Johnson-Cousins photometric system. Their location close to the celestial equator makes them accessible to telescopes in both hemispheres.

The purpose of this paper is to provide standard *UBVRI*-CCD photometry for stars in the neighbourhood of several Landolt standard stars. This will allow the use of several reduction-useful stars from a single CCD frame. The stars presented in this paper are grouped in 11 different fields, each one containing at least one Landolt star.

**Table 3.** Number of standard stars ( $N$ ) and their rms residuals ( $\sigma$ ) of each night of observation.  $V_X$  denotes  $V$  magnitude computed using colour index  $X$  in the colour-term-dependent part of the transformation equations

Night	$V_{B-V}$		$B-V$		$U-B$		$V-R$		$V-I$		$V_{V-R}$	
	$N$	$\sigma$	$N$	$\sigma$	$N$	$\sigma$	$N$	$\sigma$	$N$	$\sigma$	$N$	$\sigma$
1991-11-05	22	0.021	21	0.018	22	0.027	23	0.014	23	0.023	22	0.021
1991-11-06	21	0.019	21	0.012	20	0.035	21	0.015	13	0.020	21	0.019
1991-11-07	20	0.026	20	0.018	17	0.018	20	0.015	20	0.020	20	0.026
1991-11-08	17	0.014	15	0.009	17	0.022	13	0.011	18	0.018	16	0.010
1991-11-09	21	0.014	20	0.010	19	0.030	21	0.012	20	0.023	21	0.014
1993-10-07	19	0.017	18	0.025	16	0.043	19	0.014	19	0.022	19	0.017
1993-12-10	18	0.021	—	—	—	—	17	0.017	17	0.020	18	0.021
1993-12-11	24	0.011	24	0.022	23	0.024	—	—	—	—	—	—
1993-12-12	23	0.049	21	0.030	19	0.030	18	0.021	17	0.019	16	0.050
1993-12-15	17	0.019	17	0.016	16	0.042	15	0.013	16	0.029	17	0.019
1993-12-16	23	0.039	22	0.038	21	0.043	19	0.035	18	0.050	22	0.034
1993-12-17	23	0.037	22	0.048	23	0.035	21	0.036	19	0.027	24	0.041
1993-12-18	19	0.009	20	0.018	18	0.050	20	0.012	18	0.017	19	0.009
1993-12-19	25	0.018	23	0.028	23	0.041	23	0.016	23	0.028	23	0.025
1994-12-08	25	0.013	24	0.024	22	0.041	25	0.013	25	0.022	23	0.011
1994-12-09	19	0.028	19	0.028	17	0.035	20	0.021	19	0.021	19	0.028
1994-12-10	10	0.030	10	0.040	9	0.045	11	0.016	10	0.025	11	0.040
1994-12-11	18	0.021	20	0.012	17	0.054	20	0.015	19	0.023	19	0.022
1994-12-12	35	0.017	32	0.013	32	0.037	32	0.011	30	0.021	32	0.019

## 2. Observations and reduction

The data were acquired in the course of several campaigns devoted to obtain deep *UBVRI* Johnson-Cousins CCD photometry of open clusters and stellar associations (Cep OB3, IC 348, NGC 1750/NGC 1758; Jordi et al. 1995; Trullols & Jordi 1997; Galadí-Enríquez et al. 1998) in November 1991, October 1993, December 1993 and December 1994 at the telescopes of Centro Astronómico Hispano-Alemán (CAHA) and Observatorio Astronómico Nacional (OAN), both in Calar Alto, Almería (Spain). In these observational runs, Landolt stars were used as reference for the transformation to the standard photometric system. Table 1 shows the telescopes and chips used in each observation period. Table 2 gives the quantum efficiency of the detectors at the central wavelengths of the standard *UBVRI* filters.

The reduction from raw images to standard photometry was performed following Jordi et al. (1995), and we refer to them for a fully detailed description of the procedure. In the following paragraphs we summarize the main steps of this process.

Bias level was evaluated individually for each frame by averaging the counts of the most stable pixels in the overscan areas. The 2-D structure of the bias current was determined from a number of dark frames with zero exposure time. As pointed out in previous papers (Galadí-Enríquez et al. 1994; Jordi et al. 1995), shutter timing effects can affect the photometric results, specially when dealing with bright stars (short exposure times). The shutters of every CCD-camera were analyzed following

Galadí-Enríquez et al. (1994), and shutter effects were removed from flat-field and object frames.

The frames were processed using the ESO image processing software MIDAS. Aperture photometry was obtained using DAOPHOT, and aperture corrections were determined and applied with DAOGROW (Stetson 1987, 1990). Cross-identification of stars in different frames was performed using DAOMATCH and DAOMASTER programs (Stetson 1993).

In order to perform the transformation to the standard system, between 15 and 30 different Landolt (1983, 1992) standard stars, carefully selected to cover a wide range of spectral types and air masses, were observed each night.

The coefficients of the transformations were computed by a least square method using the instrumental magnitudes of the standard stars and their standard magnitudes and colours in the Johnson-Cousins system. Standard stars with residuals greater than  $2\sigma$  were not used in the transformation procedure. The rejected stars in each night were few (from 0 to 3 stars). Since these stars were different from night to night, the problem cannot be associated to their standard values: individual measurement problems are most probably the cause. Each rejection was checked in order not to reduce the colour range covered by the standard stars. The calculation was done in two steps, determining first the extinction coefficients (Eqs. (2) and (3) in Jordi et al. 1995) and, then fitting the remaining model parameters. Independent reductions were made for each night. The differences among instrumental coefficients from night to night within the same observing period were small and within the determined errors. The rms residuals of the standard stars are given in Table 3.

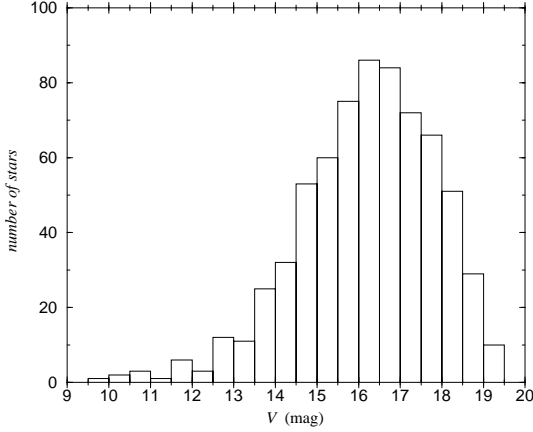


**Fig. 1.** Histogram of the sample of selected stars as a function of  $V$  magnitude

The transformation equations were applied to the instrumental data of the stars detected in the neighbourhood of Landolt standard stars. The internal errors of individual measurements were computed as described in Jordi et al. (1995), taking into account the errors in the instrumental magnitudes on the one hand, and the errors in the transformation equations on the other hand. No evidence of systematic differences between data acquired in different observational runs was found, what indicates that the transformations successfully compensated the sensitivity differences among the instrumental systems.

Thus, final magnitudes and colours were obtained by averaging the individual measurements of each star using the internal error for weighting (Jordi et al. 1995; Rosselló et al. 1985), after rejecting obviously wrong measurements (those with deviation from the mean larger than  $2\sigma$ ). The photometric errors were computed as the mean error of the mean of the final magnitudes and colours.

### 3. Selection criteria

From the detected stars, 681 have sufficient number of consistent observations to be useful as *UBVRI* secondary standard stars. The selection of these stars was done applying the following criteria.

The field of view of the detectors used in each observational run is different and, thus, not all the stars in the neighbourhood of our Landolt stars have been observed in all the observation periods. The final sample has been split into two different sets: #1 stars having at least 3 useful measurements in at least 2 different observation periods and #2 stars having at least 4 useful measurements belonging to the same period.

Among this sample, we considered as candidates to be secondary standard stars only those whose photometric errors were smaller than 0.06 mag in all bands (except from  $U - B$ , where the limit was set at 0.10 mag). Stars rejected were mainly faint ones.

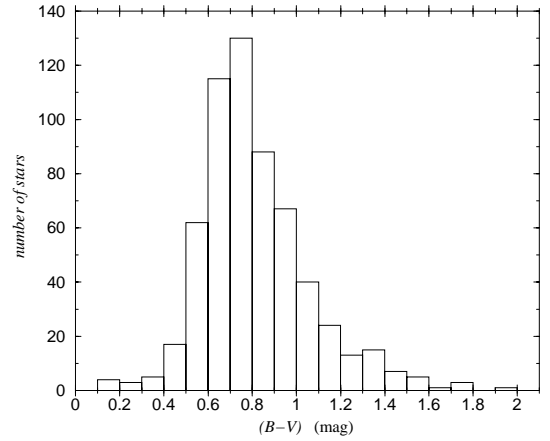


**Fig. 2.** Histogram of the sample of selected stars as a function of  $B - V$  colour index

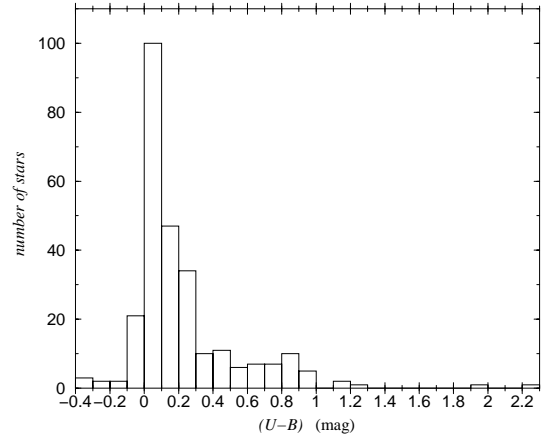


**Fig. 3.** Histogram of the sample of selected stars as a function of  $U - B$  colour index

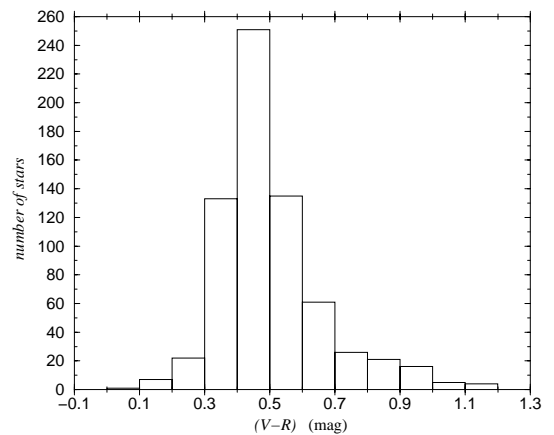


**Fig. 4.** Histogram of the sample of selected stars as a function of  $V - R$  colour index



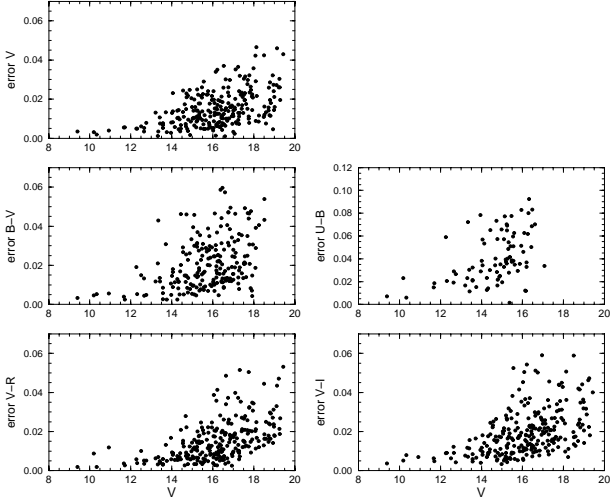


Fig. 7. Errors as a function of magnitude for the stars in set #2

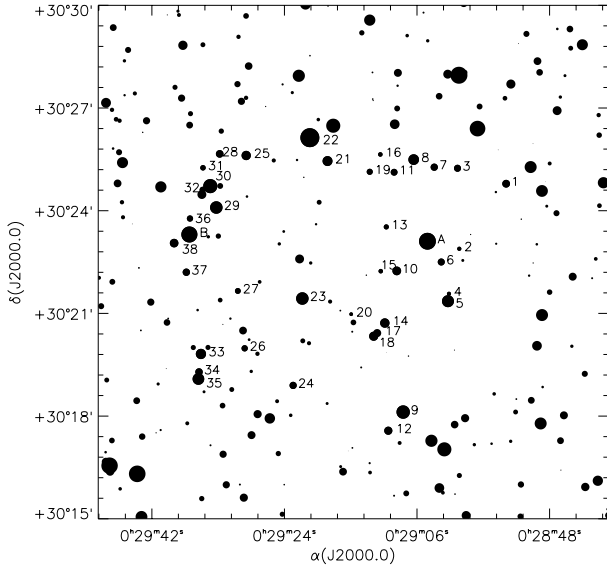


Fig. 8. Identification chart of field #1 around Landolt stars SA 44 28 (labelled “A”) and SA 44 113 (labelled “B”). Labels are placed right from the stars, except for #32, placed left

whole sample, but by intervals of two magnitudes. Inside each interval, errors increase with magnitude in a continuous manner, but this bias is very slight and only affects the rejection/acceptance of stars with larger standard deviation. Reducing the interval would lead to small number statistics in several bins.

In average, the 431 stars in set #1 were observed in 2.1 periods and have 11.7 measurements in filter *V*. The 250 stars in set #2 have, in average, 6.6 measurements in filter *V* and were observed in 1.2 periods.

#### 4. Cross-identifications and astrometry

Equatorial coordinates were computed for all selected stars using the USNO-A V2.0 catalogue (Monet et al.

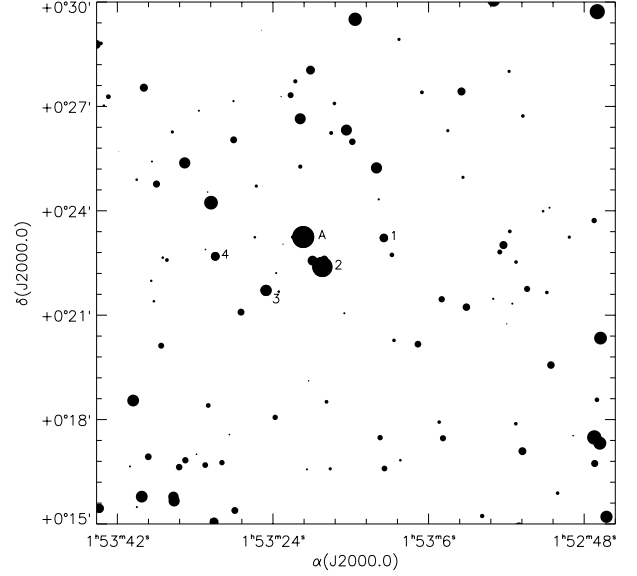


Fig. 9. Identification chart of field #2 around Landolt star SA 93 103 (labelled “A”)

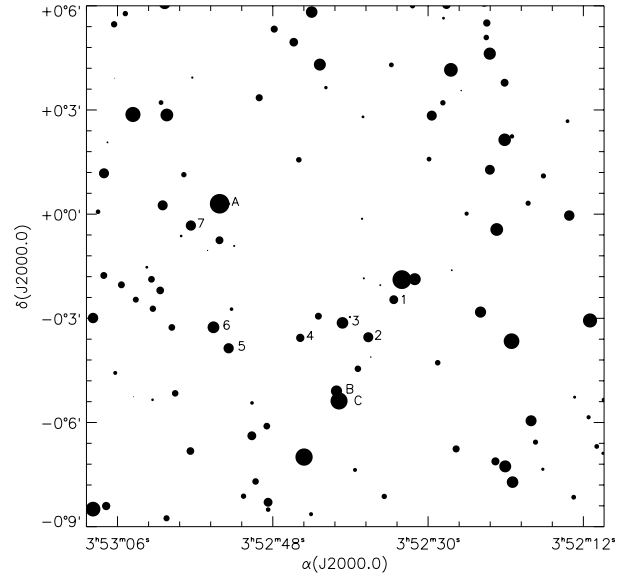


Fig. 10. Identification chart of field #3 around Landolt stars SA 95 16 (labelled “A”), SA 95 96 (labelled “B”) and SA 95 15 (labelled “C”)

1998) as reference. In each field, several stars were cross-identified with the USNO catalogue by ocular inspection. These stars were used to compute initial linear transformation equations from frame coordinates  $(x, y)$  to  $(\alpha, \delta)$ , including scale and rotation terms. The resulting equatorial coordinates were introduced into an iterative crossing-fitting procedure until convergence in the number of matched stars was reached. We did not restrict this process to the selected sample; instead, all stars detected in our CCD data were used. The final rms residual of the fittings were in both coordinates around 0.32 arcsec, in accordance with the precision claimed for

**Table 5.** *UBVRI* photometry of several Landolt standard stars. Columns give the star identifier, our photometric data (magnitude  $V$  and colour indexes  $B - V$ ,  $U - B$ ,  $V - R$  and  $V - I$ ) with their standard errors and, in the last columns, the number of observational runs ( $N_r$ ) and the number of measurements ( $N_m$ ) used for each star in each band ( $V$ ,  $B$ ,  $U$ ,  $R$  and  $I$ , in this order)

star	$V$	$B - V$	$U - B$	$V - R$	$V - I$	$N_r$	$N_m$	$N_r$	$N_m$	$N_r$	$N_m$	$N_r$	$N_m$	$N_r$	$N_m$
44 028	11.329±0.002	0.726±0.001	0.200±0.004	0.394±0.001	0.764±0.002	4	30	4	16	4	34	4	23	4	35
44 113	11.713±0.006	1.206±0.002	0.996±0.019	0.667±0.003	1.229±0.005	1	9	1	7	1	10	1	7	1	9
76 280	12.670±0.004	0.925±0.006	0.728±0.015	0.531±0.004	0.989±0.002	3	16	3	15	3	14	3	12	2	8
76 281	12.235±0.001	0.537±0.003	-0.015±0.007	0.301±0.003	0.588±0.007	3	8	3	12	3	14	3	11	3	12
93 103	8.834±0.001	1.179±0.001	1.182±0.001	0.582±0.001	1.103±0.002	2	3	2	3	2	3	2	3	3	4
95 016	14.306±0.010	1.287±0.008	—	0.802±0.006	1.483±0.008	1	4	1	4	0	0	1	4	1	4
95 096	9.995±0.001	0.155±0.001	0.041±0.001	0.085±0.001	0.190±0.001	2	3	2	3	2	3	2	3	2	3
96 405	10.664±0.005	1.291±0.007	1.505±0.008	0.653±0.002	1.214±0.004	3	12	3	13	3	11	3	12	3	14
96 406	9.296±0.003	0.213±0.002	0.125±0.004	0.116±0.005	0.242±0.005	3	11	3	10	3	15	3	15	3	15
98 185	10.544±0.002	0.187±0.003	0.108±0.003	0.118±0.004	0.247±0.003	3	12	3	12	3	9	3	14	3	11
98 193	10.021±0.002	1.166±0.005	1.170±0.005	0.613±0.003	1.153±0.003	3	8	3	14	3	9	3	13	3	11
98 650	12.277±0.003	0.157±0.004	0.121±0.006	0.076±0.002	0.175±0.005	4	18	4	18	3	18	3	15	3	18
98 653	9.533±0.001	0.024±0.002	-0.119±0.001	-0.003±0.003	0.012±0.001	2	3	2	3	3	3	4	14	3	3
98 667	8.382±0.001	0.041±0.003	-0.337±0.009	0.083±0.007	0.170±0.005	2	3	4	10	3	11	3	14	3	12
98 670	11.930±0.002	1.351±0.007	1.335±0.008	0.722±0.002	1.371±0.001	4	20	4	22	3	18	3	17	3	13
98 671	13.385±0.003	0.963±0.003	0.800±0.013	0.576±0.002	1.066±0.005	3	15	3	14	3	17	3	16	3	19
98 682	13.747±0.002	0.653±0.006	0.104±0.019	0.361±0.005	0.696±0.006	3	9	3	13	3	16	3	17	3	15
98 685	11.945±0.003	0.488±0.005	0.050±0.019	0.283±0.004	0.566±0.004	2	14	2	12	2	16	2	16	2	14
99 438	9.395±0.006	-0.164±0.005	-0.645±0.014	-0.059±0.003	-0.136±0.003	2	7	2	5	2	8	2	7	1	6
99 447	9.395±0.003	-0.060±0.003	-0.210±0.007	-0.036±0.002	-0.063±0.004	1	5	1	4	1	6	1	5	1	6
100 267	13.035±0.003	0.492±0.003	-0.049±0.013	0.310±0.005	0.610±0.003	2	8	2	10	2	10	2	8	2	10
100 269	12.367±0.003	0.550±0.006	-0.006±0.009	0.340±0.004	0.662±0.002	2	7	2	9	2	9	2	8	2	10
113 274	8.824±0.001	0.484±0.002	0.012±0.002	0.279±0.002	0.547±0.004	2	3	2	8	1	6	2	7	2	9
113 276	9.065±0.001	0.653±0.003	0.189±0.004	0.361±0.001	0.684±0.005	2	3	2	7	3	10	2	3	2	9
114 750	11.926±0.006	-0.058±0.005	-0.314±0.011	0.029±0.001	-0.027±0.003	3	8	4	10	4	13	3	3	2	3
GD 71	13.035±0.002	-0.243±0.004	-1.083±0.008	-0.134±0.002	-0.314±0.002	2	34	2	34	2	32	2	33	2	30

**Table 6.** Individual differences among Landolt’s data and our photometry in the sense *this work*-minus-*Landolt*

star	$V$	$B - V$	$U - B$	$V - R$	$V - I$
44 028	0.002	-0.012	-0.018	0.001	0.002
44 113	0.006	0.000	-0.031	0.004	-0.005
76 280	0.001	0.009	0.013	-0.006	-0.015
76 281	-0.007	0.018	-0.056	0.002	-0.010
93 103	0.003	0.018	0.025	-0.003	-0.001
95 016	-0.007	-0.019	—	0.006	0.010
95 096	-0.019	0.008	-0.027	0.006	0.018
96 405	0.002	0.013	-0.001	0.001	0.007
96 406	-0.004	-0.007	-0.023	0.000	0.005
98 185	0.007	-0.016	-0.006	0.006	0.009
98 193	-0.006	-0.009	0.007	-0.003	-0.001
98 650	0.006	0.000	0.011	-0.004	0.009
98 653	-0.005	0.028	-0.022	-0.010	-0.002
98 667	0.004	0.013	-0.001	0.012	0.021
98 670	0.000	-0.005	0.022	-0.001	-0.004
98 671	0.000	-0.005	0.081	0.001	-0.005
98 682	-0.002	0.021	0.006	-0.005	-0.021
98 685	-0.009	0.025	-0.047	-0.007	-0.004
99 438	-0.005	-0.009	0.074	0.001	0.007
99 447	-0.020	0.011	0.007	-0.005	0.011
100 267	0.007	0.006	-0.016	0.004	0.095
100 269	0.016	-0.007	0.005	0.008	0.079
113 274	-0.007	0.004	0.009	-0.006	-0.008
113 276	-0.009	0.006	0.008	0.004	-0.008
114 750	0.013	-0.020	0.043	-0.001	-0.040
GD 71	0.003	0.006	0.024	0.003	-0.012

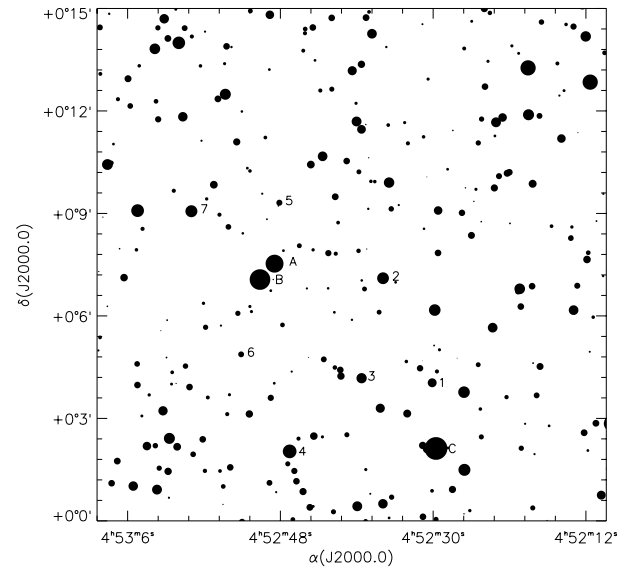


**Fig. 11.** Identification chart of field #4 around Landolt stars SA 96 405 (labelled “A”), SA 96 406 (labelled “B”) and SA 96 393 (labelled “C”)

USNO-A V2.0 (around 0.25 arcsec in each coordinate) and with the deviations that may arise from proper motions due to epoch differences.

Several discordant matches with USNO-A V2.0 (further than 1 arcsec) were due to relatively high proper-motion stars. Other discordant matches were in

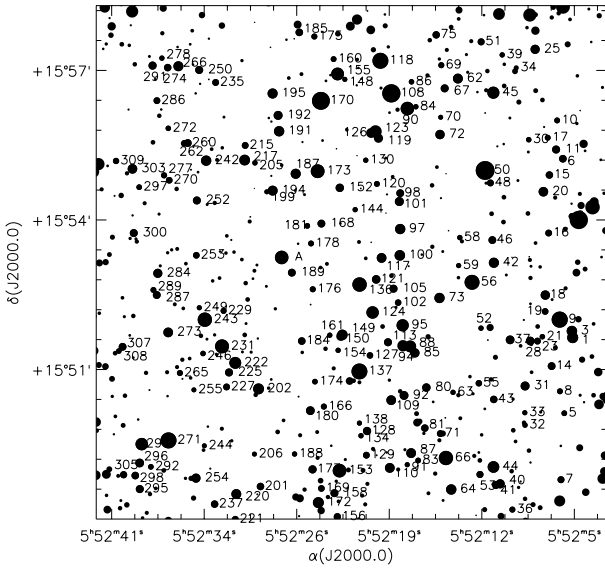


**Fig. 12.** Identification chart of field #5 around Landolt star GD 71 (labelled “A”). Only stars brighter than  $V = 17.5$  mag are labelled. Labels are placed right from the stars, except for #19, #126 and #181 that are placed left, #28, #53, #90, #94, #262, #274 and #291 placed down and #52, #113, #161 and #305 placed up

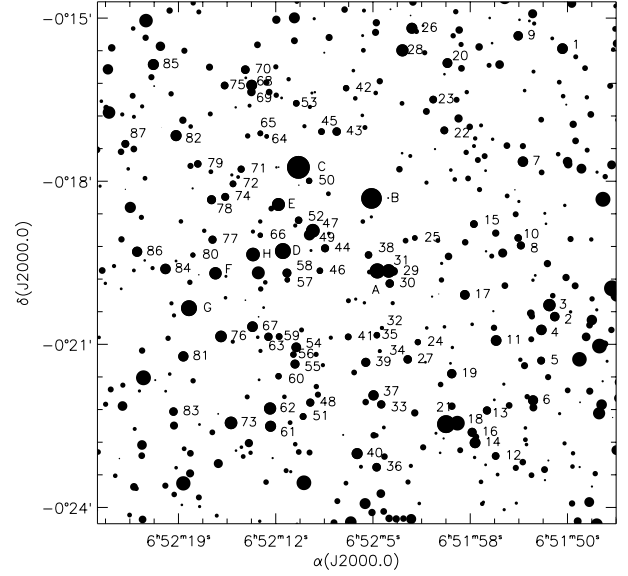


**Fig. 14.** Identification chart of field #7 around Landolt stars SA 98 650 (labelled “A”), SA 98 653 (labelled “B”), SA 98 667 (labelled “C”), SA 98 670 (labelled “D”), SA 98 671 (labelled “E”), SA 98 682 (labelled “F”), SA 98 685 (labelled “G”) and SA 98 676 (labelled “H”). Labels are placed right from the stars, except for #21 and #45, placed up, and SA 98 650 (A) and #63, placed down

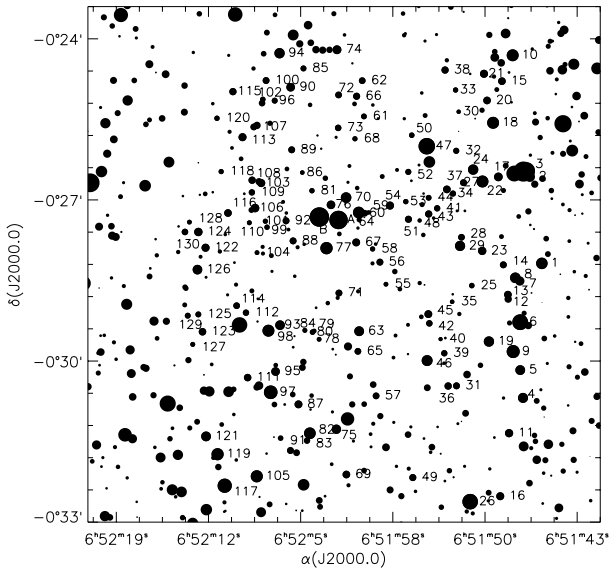


**Fig. 13.** Identification chart of field #6 around Landolt stars SA 98 185 (labelled “A”) and SA 98 193 (labelled “B”). Labels are placed right from the stars, except for #36, #51, #64, #110, #129 and #130, all of them placed down, and SA 98 193 (B), #17, #24, #54, #84, #102, all of them placed up

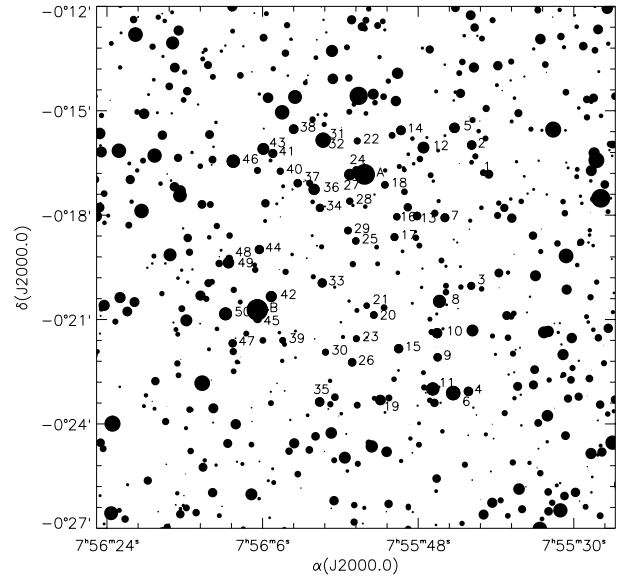


**Fig. 15.** Identification chart of field #8 around Landolt stars SA 99 438 (labelled “A”) and SA 99 447 (labelled “B”). Labels are placed right from the stars, except for #24 and #35, placed up

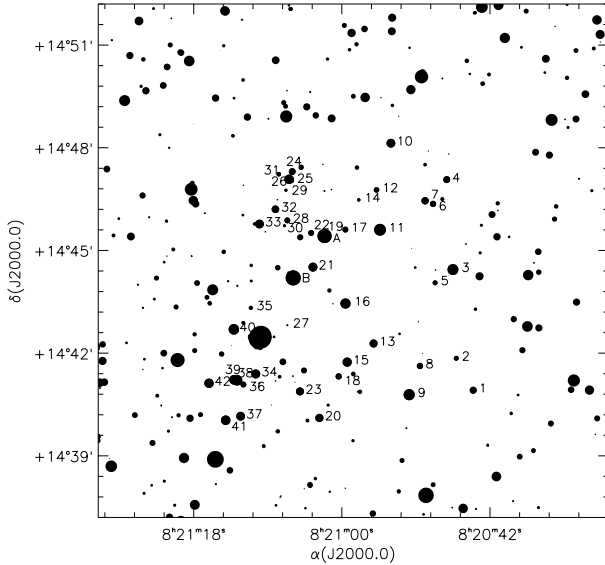


**Fig. 16.** Identification chart of field #9 around Landolt stars SA 76 280 (labelled “A”) and SA 76 281 (labelled “B”). Labels are placed right from the stars, except for #24, #38 and #39, placed up, and for #26 and #31, placed left

every case related to double stars not resolved in USNO plate scans, but well-separated in our CCD data. In these cases, the match was assigned to the primary (brighter) component.

The positions given for our stars were determined by applying the transformation equations from  $(x, y)$  to  $(\alpha, \delta)$  (J2000.0 equinox, at the mean epoch of the observations). These equatorial coordinates were used to match our stars with AC 2000 catalogue (Urban et al. 2000). Due to the brighter limiting magnitude of AC 2000, few of our stars have a cross-identification with this catalogue.

## 5. Description of the sample

The astrometric positions were used to assign individual identifiers to the stars in our sample. First of all, the different fields were numbered from 1 to 11 following the order of the increasing mean right ascension. Inside each field, stars were numbered following the order of the increasing right ascension.

Table 4 contains both data sets #1 and #2. This table (available also in electronic form) contains: field number and star number inside that field, J2000.0 equatorial coordinates, photometry ( $V$ ,  $B - V$ ,  $U - B$ ,  $V - R$ ,  $V - I$ , each quantity followed by its internal error), number of observational runs in which useful data were obtained, number of useful measurements in  $V$ , cross-identification with USNO-A V2.0 catalogue, and notes. Notes give further cross-identifications with AC 2000, Tycho and Hipparcos (ESA 1997) catalogues (matches with Tycho and Hipparcos are directly drawn from AC 2000) and the

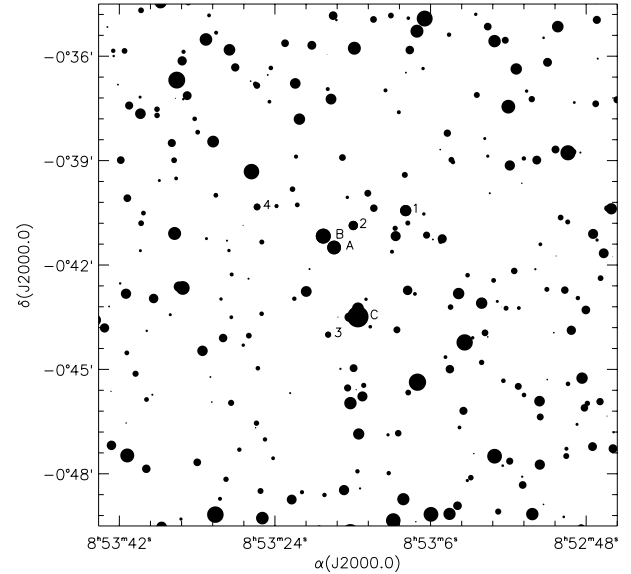


**Fig. 17.** Identification chart of field #10 around Landolt stars SA 100 267 (labelled “A”), SA 100 269 (labelled “B”) and SA 100 162 (labelled “C”)

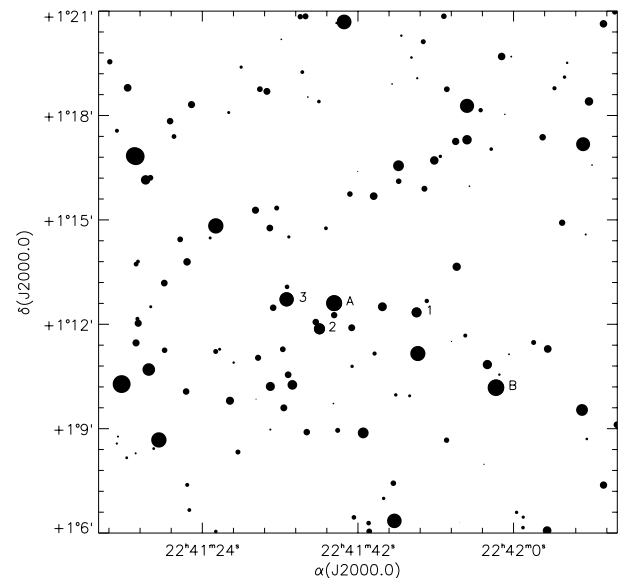


**Fig. 18.** Identification chart of field #11 around Landolt stars SA 114 750 (labelled “A”) and SA 114 654 (labelled “B”)

Selected Areas. Stars belonging to set #2 are marked with an asterisk in the notes. Stars from set #1 are not marked.

The colour index and apparent visual magnitude distributions of the stars included in sets #1 and #2 are shown in Figs. 1 to 5. The photometric errors as a function of apparent visual magnitude are given in Fig. 6 for set #1 and in Fig. 7 for set #2.

Table 5 includes our photometric values for several Landolt standard stars. Individual differences with Landolt’s photometry are given in Table 6. The rms of the residuals with the values given by Landolt (1983, 1992) are  $\sigma_V = 0.009$  mag,  $\sigma_{B-V} = 0.014$  mag,  $\sigma_{U-B} = 0.032$  mag,



$\sigma_{V-R} = 0.005$  mag and  $\sigma_{V-I} = 0.013$  mag, which are of the same order as the residuals quoted in Table 3.

Figures 8 to 18 display identification charts for our 11 fields. Figure captions identify each field by its number, and the stars in our sample are labelled with the same numbering system used in Table 4. Landolt stars are marked with capital letters, and their identifiers are given in figure captions.

## 6. Conclusions

We have provided a set of 681 new secondary standard stars which are useful for the transformation of instrumental *UBVRI*-CCD data to the standard Johnson-Cousins system. These stars cover a wide interval in visual magnitude as well as in colour indexes. They are distributed in 11 different fields, all of them located around Landolt (1983, 1992) primary standards and mainly in the interval from 5 to 8 hours in right ascension.

*Acknowledgements.* The 1.23 m telescope is operated by the Max-Planck Institut für Astronomie at Centro Astronómico Hispano-Alemán, Calar Alto, Almería, Spain. The 1.52 m telescope is operated by Observatorio Astronómico Nacional at Calar Alto, Almería, Spain. This work was supported by the CICYT under contract ESP95-0180. D.G.-E. acknowledges partial support from Área de Formación del Instituto Nacional de Técnica Aeroespacial “Esteban Terradas” (Becas de Formación en Astrobiología). The authors thank Dr. Leonel Gutiérrez (UNAM) for his comments on CCD detectors.

## References

- ESA, 1997, The Hipparcos and Tycho Catalogues, ESA-SP 1200
- Galadí-Enríquez D., Jordi C., Trullols E., 1994, in *New Developments in Array Technology and Applications*, Philip A.G.D. (ed.) Proc. IAU Symp. 167, 327
- Galadí-Enríquez D., Jordi C., Trullols E., Ribas I., 1998, *A&A* 333, 471
- Jordi C., Galadí-Enríquez D., Trullols E., Lahulla F., 1995, *A&AS* 114, 489
- Landolt A.U., 1983, *AJ* 88, 439
- Landolt A.U., 1992, *AJ* 104, 340
- Monet D., Bird A., Canzian B., et al., 1998, USNO-A V2.0: a Catalog of Astrometric Standards, U.S. Naval Observatory, Washington DC
- Rosselló G., Calafat R., Figueras F., et al., 1985, *A&AS* 59, 399
- Stetson P.B., 1987, *PASP* 99, 191
- Stetson P.B., 1990, *PASP* 102, 932
- Stetson P.B., 1993, Proc. IAU Coll. 136: *Stellar Photometry, Current Techniques and Future Developments*. Cambridge University Press, Cambridge, p. 291
- Trullols E., Jordi C., 1997, *A&A* 324, 549
- Urban S.E., Corbin T.E., Wicoff G.L., 2000, AC 2000: the Astrographic Catalogue on the Hipparcos System, U.S. Naval Observatory, Washington DC